Molecular Crystals and Liquid Crystals
Publication details, including instructions for authors and subscription information:
http://www.tandfonline.com/loi/gmcl18

X-Ray Diffraction From Free Standing Films of Hexatic Smectic Liquid Crystals

A. S. Cherodian [a] & R. M. Richardson [a]
[a] School of Chemistry, University of Bristol, Cantock's Close, Bristol, BS8 1TS, U.K.
Version of record first published: 24 Sep 2006.

To cite this article: A. S. Cherodian & R. M. Richardson (1991): X-Ray Diffraction From Free Standing Films of Hexatic Smectic Liquid Crystals, Molecular Crystals and Liquid Crystals, 196:1, 115-131

To link to this article: http://dx.doi.org/10.1080/00268949108029691

Mol. Cryst. Liq. Cryst., 1991, Vol. 196, pp. 115–131
Reprints available directly from the publisher
Photocopying permitted by license only

Printed in the United States of America

X-Ray Diffraction From Free Standing Films of Hexatic Smectic Liquid Crystals

A. S. CHERODIAN and R. M. RICHARDSON

School of Chemistry, University of Bristol, Cantock's Close, Bristol BS8 1TS, U.K.

(Received for publication July 25, 1990; in final form October 18, 1990)

A selection of novel materials exhibiting smectic polymorphism has been studied by X-ray diffraction. The smectic A and smectic C phases were generally identified from the diffraction patterns of magnetically aligned samples in Lindemann tubes. Some of the crystal smectic phases were identified by indexing the diffraction lines from the powder patterns. However it was not possible to distinguish between the hexatic phases (i.e., S_B, S_F and S_I) by diffraction from magnetically aligned samples in Lindemann tubes because sufficiently large monodomains could not be obtained. We therefore prepared monodomain, free-standing films and recorded diffraction patterns. The distribution of scattered X-ray intensity amongst the six equatorial spots is characteristic of the phase if the beam is perpendicular to the smectic layers. However, if the beam is not perpendicular, identifying the phase is more complicated. We have therefore calculated the diffraction pattern expected for any unit cell and angle of incidence and used the results to assist in identifying the phases.

Keywords: smectic polymorphism, hexatic liquid crystal, X-ray diffraction, free standing film, computed diffraction pattern

1. INTRODUCTION

The free-standing film of a liquid crystal is an ideal system for studying the structure and properties of various smectic phases.[1-10] The technique provides uniform, large area (up to 1 cm^2) films in which the layers are stacked parallel to the surface of the film. Two methods have been used to prepare these films. In the original method used by Moncton and Pindak,[1] the films are drawn over a hole in a metal plate when the liquid crystal is in the smectic A (S_A) or smectic C (S_C) phase. The thickness of the film can be varied from two layers to several hundred layers. Prezdmojski and Gierlotka[9] prepared thicker films (0.1–1.0 mm) by packing the hole with the liquid crystal and then heated the sample to its nematic or isotropic phase. The films form spontaneously on cooling. The films were usually reported to be mosaic, consisting of many domains disordered about the axis perpendicular to the film. Single-domain samples were prepared by the application of an external magnetic[6,7,9] or electric[9,10] field. Here we report a systematic X-ray study of monodomain free-standing films of a selection of materials supplied by Professor G. W. Gray and Dr. D. Lacey of Hull University. The main object was to establish the nature of the hexatic phases. It was found necessary to use suspended films as

well as Lindemann tube samples in order to identify the hexatic phase unambiguously.

2. DIFFRACTION GEOMETRY

In the hexatic phases,[11,12] the molecular packing is essentially hexagonal in the plane normal to the molecular axes. The molecules may be oriented either normal to the smectic layers (hexatic B phase) or tilted by a fixed angle with respect to the smectic layer normal (S_I and S_F phases). This gives rise to a local structure which is genuinely hexagonal for the hexatic B phase and pseudo-hexagonal, *c*-centered monoclinic for the S_F and S_I phases. The lattice axes in these phases have long range order of direction (bond orientational order). Fig. 1 shows diagrammatically the real and reciprocal lattices of S_I and S_F phases.[11] In the S_I phase, the molecules are tilted towards the apex of the pseudo-hexagonal lattice, whereas in the S_F phase the tilt direction is towards the edge.

The reciprocal lattice of a hexatic phase contains six diffraction maxima in the *hk*0 plane which has pseudo-hexagonal symmetry (only the lowest *hk*0 reflections are observed). The maxima are in the shape of diffuse bars along the c^* direction. Since there is no positional correlation of the molecules between the smectic layers, the strength variation of the scattering function along the bars depends only upon

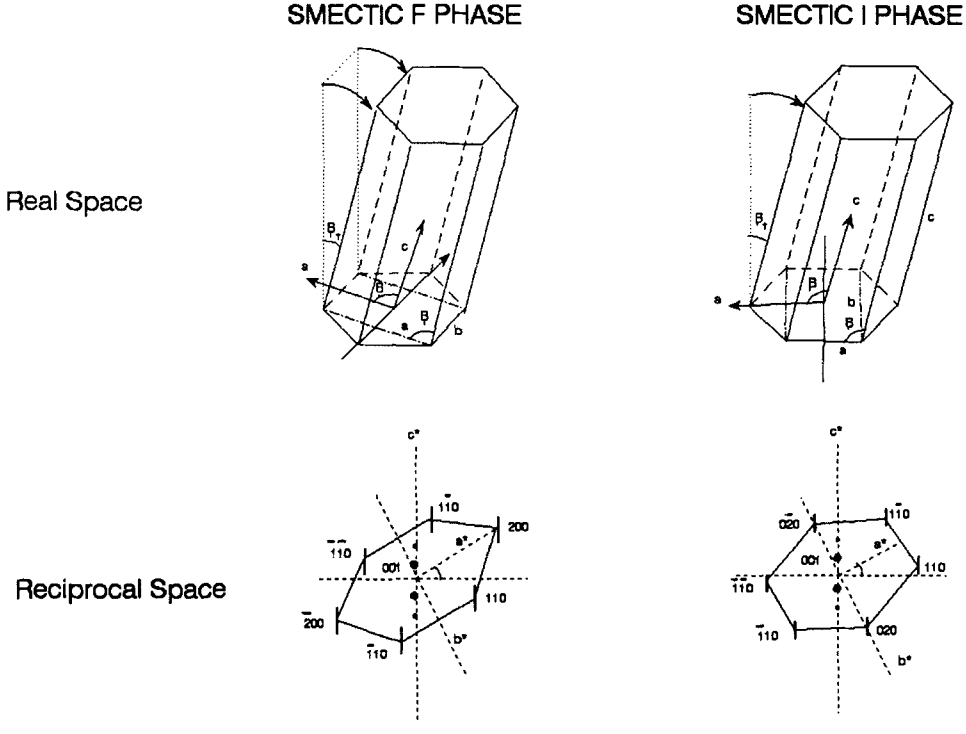

FIGURE 1 Schematic representations of the real (upper) and reciprocal (lower) lattices of the S_I and S_F phases. The molecules are arranged with the molecular long axes parallel to *c*, with pseudo-hexagonal packing of the molecules in the plane perpendicular to *c*.

the molecular form factor. This has a maximum for scattering vectors ($\vec{Q}$) in a plane through the origin, perpendicular to the molecular axis. The strength of the scattering function is therefore a maximum at the point where the rods pass through this plane and it decreases (monotonically at first) for scattering vectors out of this plane. Diffraction spots are observed at the points in reciprocal space, where the Ewald sphere intersects the scattering function. Hence in the case of the orthogonal hexatic B phase, if the X-ray beam is perpendicular to the smectic layers, the molecular form factor is parallel to the plane of the smectic layers and the diffraction pattern will have six spots of equal intensity. Fig. 2 illustrates the diffraction geometry of a tilted hexatic (S_I or S_F) phase in which the molecular form factor is tilted with respect to the plane of the smectic layers, when the X-ray beam is perpendicular to smectic layers. Effectively, some of the six diffraction maxima will be weaker or missing. The diffraction pattern is characteristic of the phase, because it is possible to determine whether the reciprocal lattice net is tilted towards the edge of the hexagon (S_I phase) or tilted towards the apex of the hexagon (S_F phase). All six diffraction spots are observed with equal intensity when the sample is rotated such that the Ewald sphere intersects all three Freidel pairs as shown by the dashed line in Fig. 2; this will occur only for one direction of the incident X-ray beam which is nearly parallel to the direction of the molecular long axes.

3. IDENTIFICATION OF HEXATIC SMECTIC PHASES

If samples with well aligned layers, but "fibre averaged" about c^* can be obtained by magnetic alignment, it is generally simple to distinguish between the hexatic smectic phases by X-ray diffraction with the incident beam parallel to the layers.[11] If such well aligned samples cannot be prepared, an alternative is to use free standing liquid crystal films with the incident beam perpendicular to the layers. In principle, the S_B should give a hexagon of 6 equal diffraction spots, the S_I should give a pattern with a mirror plane running through opposite edges of the hexagon, and the S_F should give a pattern with a mirror plane running through two apices of the hexagon. However, we have simulated the diffraction patterns for off-perpendicular incidence and have found that small deviations can give misleading diffraction patterns. The calculation, outlined below, has been used to explore the effect of these deviations and establish some reliable rules for phase identification.

i) Since there is little or no positional correlation of molecules between the smectic layers in a hexatic phase, the scattering can only occur for $\overline{Q}$ values that form a 2-dimensional array of rods oriented parallel to the layer normal.

ii) The points in reciprocal space where the Ewald sphere intersects these lines give rise to the observed diffraction spots. The distances of these intersections from the origin gives the $\overline{Q}$ values for the reflection.

iii) The intensity of the diffraction spots depends on the molecular form factor. This is a Fourier transform of a rod shaped molecule and will have its highest value in a plane perpendicular to the molecular axis. The value of the molecular form factor at the intersections have been calculated assuming a rod with a gaussian distribution (standard deviation = $l/\sqrt{12}$) of electron density along its length.

iv) The angle of incidence of the X-ray beam to the smectic layers is defined by

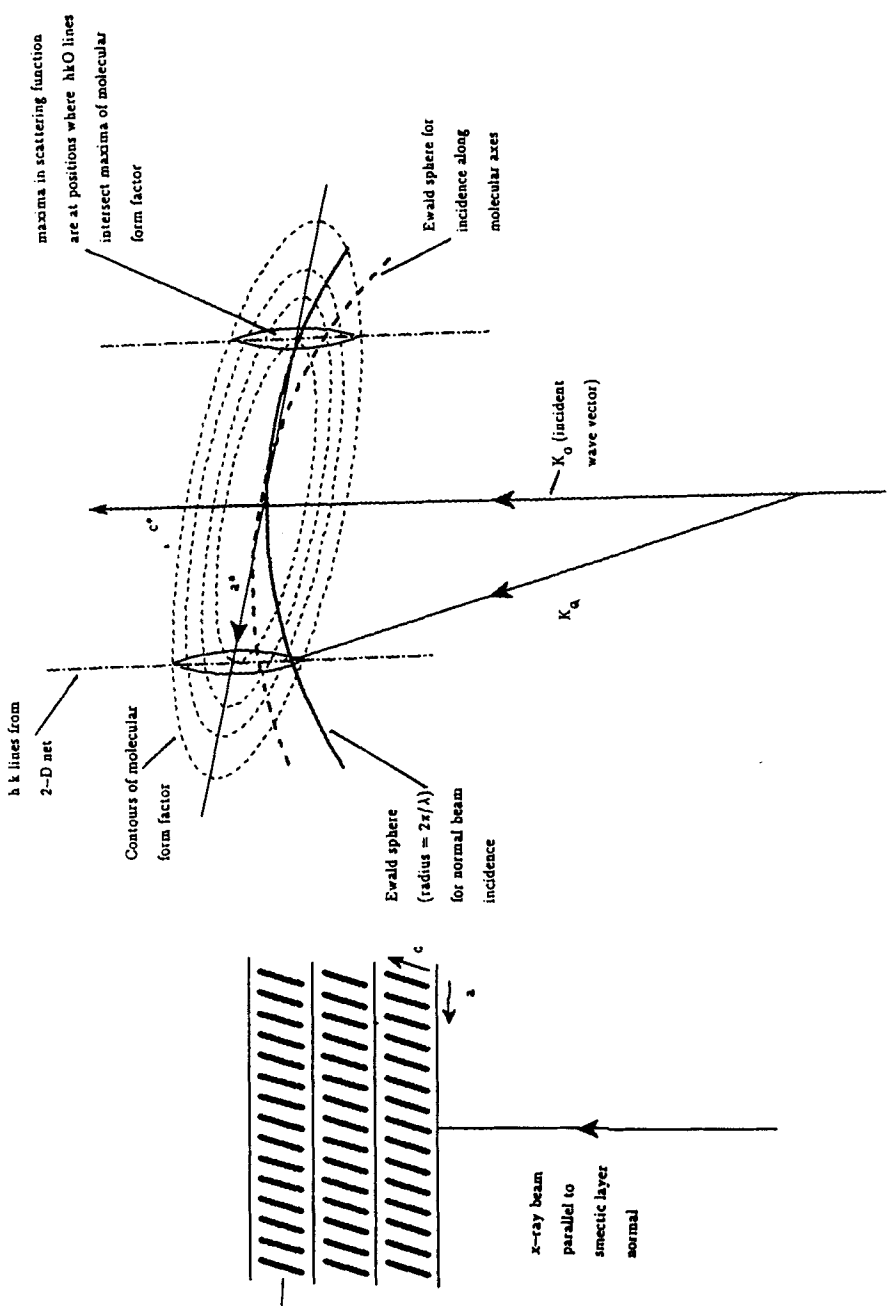

FIGURE 2 Diffraction geometry of a tilted hexatic phase when the X-ray beam is (*a*) parallel to the smectic layer normal and, (*b*) parallel to the molecular axis; diffraction spots are observed where the Ewald sphere intersects the maxima in the scattering function.

two angles 'θ' and 'ϕ', where θ is the angle between the X-ray beam and the smectic layer normal and ϕ is the angle between the X-ray beam and the *ac* plane in real space.

v) Fig. 3 shows some typical results where the radius is proportional to the optical density of the diffraction spot. These calculations have been done for a range of angles of incidence for different unit cells of hexatic B, F and I phases. The main conclusions from the calculations are the following:

a) If the beam is really perpendicular to the smectic layers, the pattern observed is characteristic of the phase for a given X-radiation. The S_F phase generally has a pattern which has a mirror plane through a diffraction spot (similar to pattern B in Fig. 4) and the S_I phase has a mirror plane between two diffraction spots (see pattern A in Fig. 3), while the hexatic B phase has six spots of equal intensity. Rotation of the sample about the beam axis will result in the rotation of the diffraction pattern through the same angle, and without any change in the intensity of the spots. This is particularly important when distinguishing between a low tilted S_F, S_I phase and a hexatic B phase where the smectic layers are not perfectly normal to the beam.

b) Small deviations from perpendicular can make it difficult to distinguish the phases (see patterns C and D in Fig. 4).

c) In the S_I or S_F phase, rotation of the sample until six spots are observed means that the incident beam is nearly (but not exactly) parallel to the molecular long axes. A measurement of the angle of rotation from the position where the beam is perpendicular to the position where six equal spots are observed (β_m) is slightly less than the real value of β_t, the tilt angle of the molecular long axis with respect to the layer normal. Fig. 3 shows that the six spots of equal intensity occur at $\theta \sim 13\frac{1}{2}°$, whereas the unit cell is tilted by 15°. The difference between β_t and β_m arises because the Ewald sphere does not coincide at the same position on opposite maxima due to its curvature, and hence the difference will depend on λ, the wavelength of the X-radiation.

d) In this position (six equal intensity spots), there is a displacement of the hexagonal diffraction pattern of the tilted hexatic phases as shown in Fig. 5. This can be clearly observed (see Fig. 7) and can be a very useful confirmation of phase identity, provided the tilt angle is not too low.

4. X-RAY DIFFRACTION STUDIES; EXPERIMENTAL

The compounds studied are listed in Table I.

The transition temperatures and possible phase sequences were determined by optical and thermal analysis by Professor Gray's group at Hull University. All the diffraction patterns were recorded on flat plate film apparatus mounted on a sealed source tube. Exposure times varied between 3–12 h. Compound **VI**, terephthalylidene-*bis*-4-n-nonylanaline (TBNA) was also included because it was believed to exhibit a smectic F phase.[13]

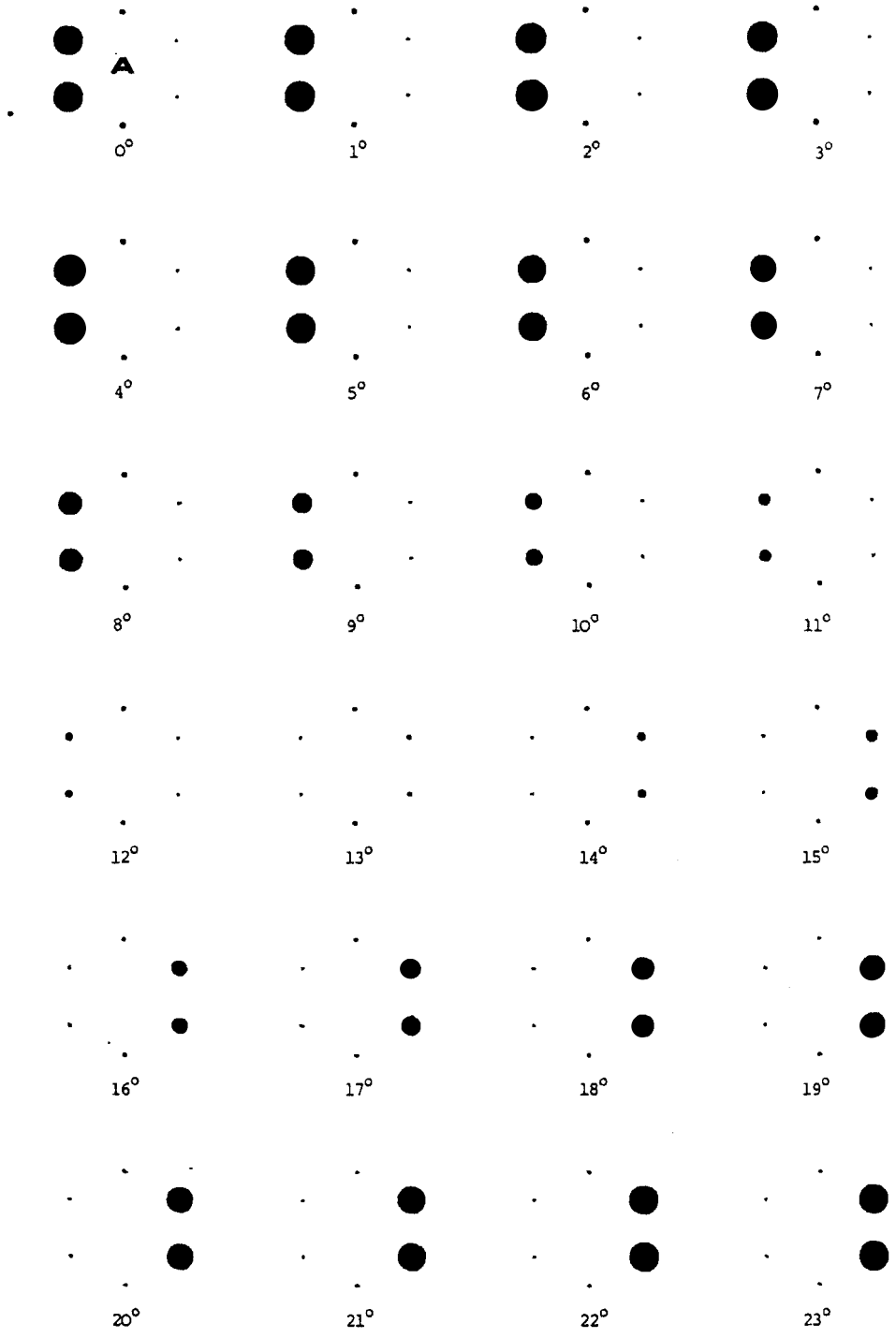

FIGURE 3 Simulation of diffraction patterns from an S_I phase obtained with Cu $K\alpha$ radiation on varying θ, the angle between the X-ray beam and the smectic layer normal, in the *ac* plane ($\phi = 0$); lattice parameters are assumed as $a = 5.432$ Å, $b = 9.088$ Å, $c = 36.543$ Å and $\beta = 105°$.

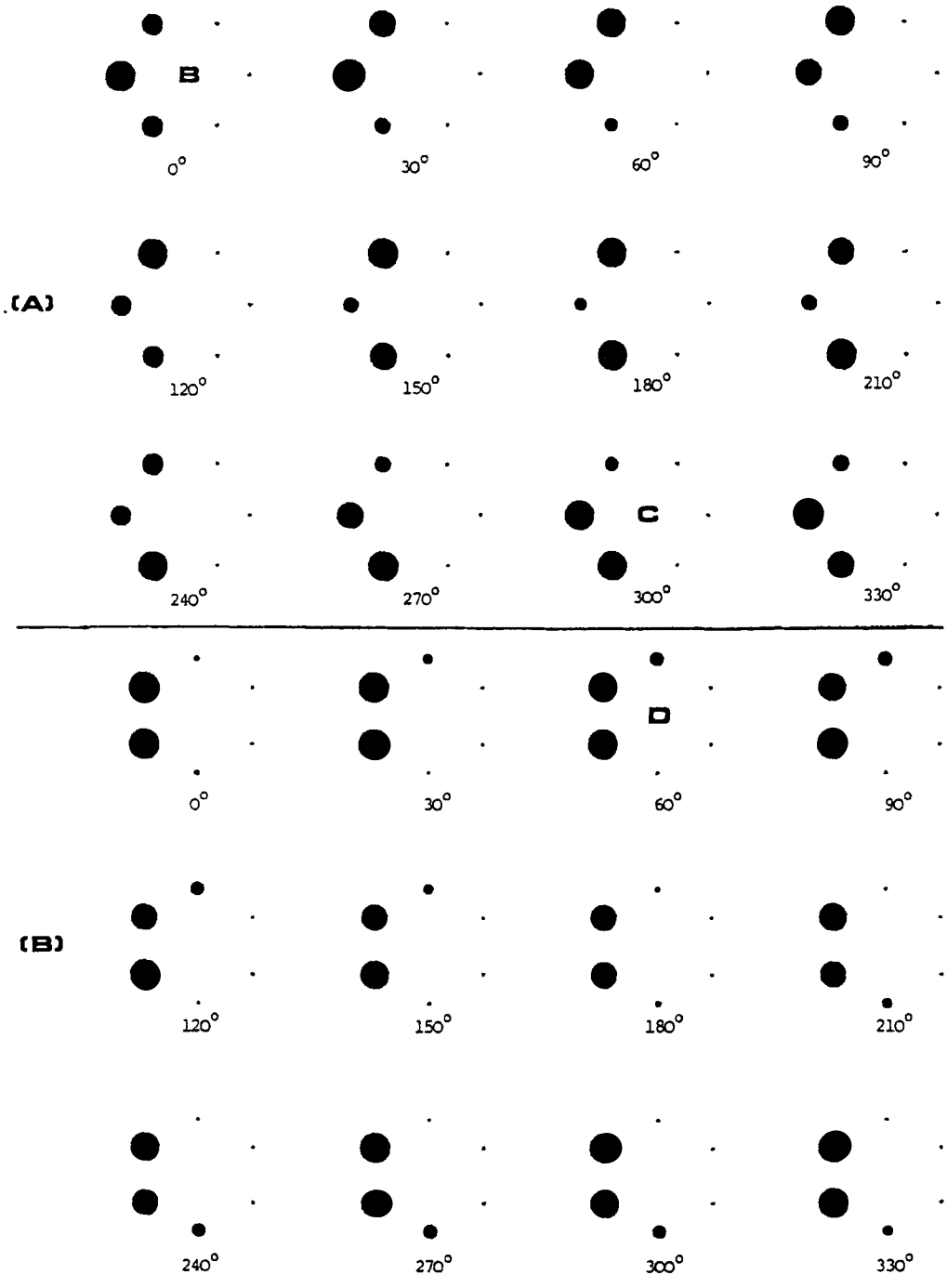

FIGURE 4 Calculations of intensities of diffraction spots with Cu $K\alpha$ radiation for (*a*) the S_F phase when the sample is rotated about an axis parallel to the X-ray beam (ϕ is varied) and with $\theta = 4°$; lattice parameters are assumed to be $a = 5.432$ Å; $b = 9.088$ Å; $c = 36.543$ Å and $\beta = 105°$; (*b*) the S_I phase obtained on varying ϕ; $\theta = 2°$; lattice parameters are assumed to be $a = 9.088$ Å; $b = 5.068$ Å; $c = 36.543$ Å and $\beta = 105°$.

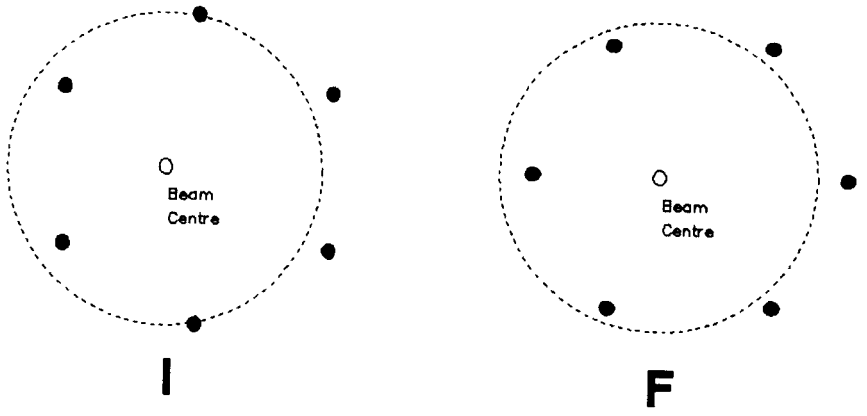

FIGURE 5 This shows schematically the distortion of the six spot pattern.

4.1 Lindemann tube samples

Each sample was contained in 1.0 mm Lindemann glass tube. The sample was then placed in a heater and the temperature controlled within 1°C using a Eurotherm controller. The samples were heated to their isotropic state and gradually cooled at 1°C per 3 h in a 1 tesla magnetic field. Diffraction patterns were recorded using nickel filtered copper ($K\alpha$) radiation with the X-ray beam perpendicular to the direction of the magnetic field. Patterns were recorded at several temperatures within each phase range in order to investigate the variation of layer spacing and tilt angle with temperature.

4.2 Free-standing films

The method used for the preparation of the free-standing film was similar to that used by Przedmojski and Gierlotka.[9,10] The liquid crystals, all in powder form at room temperature, were carefully packed into a 2 mm hole made in a brass plate of 0.7 mm thickness. This was done by hand using a suitable flat instrument. The sample holder was then placed in an oven and gradually heated (any gaps that appeared during heating were filled). The sample was heated to within 1–3°C of the smectic-isotropic transition, when the sample begins to melt and flow, leaving behind a thin film. At this stage the temperature was immediately dropped by 3–5°C. This was done to prevent the film from rupturing, furthermore it was observed to affect the thickness of the films. The oven was then placed in a strong magnetic field (2.3 T) with the film perpendicular to the direction of the magnetic field. The samples were cooled gradually at a rate of 1°C/3 h to the required phase. The cooling rate was increased to 1°C/h between phase transitions. At the required temperature, the samples were removed from the magnetic field and mounted on to the diffractometer. Well aligned samples were generally obtained. The oven used by us was designed to facilitate the rotation of the film about an axis in the plane of the film. This enabled us to record diffraction patterns at different angles of incidence. X-ray patterns were recorded using nicked filtered copper ($K\alpha$) radiation and/or zirconium filtered molybdenum ($K\alpha$) radiation. The sample thick-

TABLE I

I	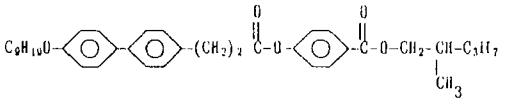	K $^{62.0}$ S_I $^{76.6}$ S_C $^{105.2}$ S_A $^{123.8}$ I
II	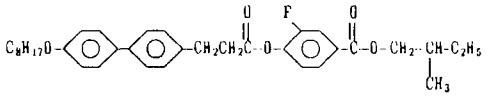	K ^{52} S_K ^{57} S_I ^{81} S_C ^{84} S_A ^{110} I
III	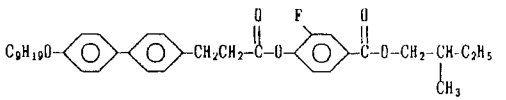	K $^{49.0}$ S_K $^{53.0}$ S_I $^{75.4}$ S_C $^{94.5}$ S_A $^{109.4}$ I
IV	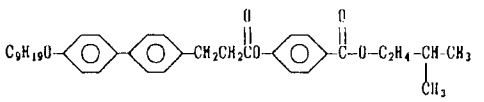	K $^{96.0}$ S_I $^{103.2}$ S_C $^{119.0}$ S_A $^{130.5}$ I
V	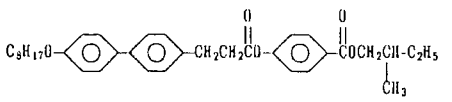	K $^{62.0}$ S_I $^{89.5}$ S_C ^{105} S_A ^{127} I
VI	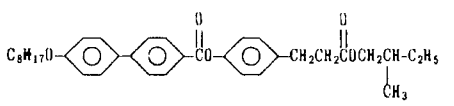	K $\xrightarrow{45.6}$ S_J $^{89.2}$ S_C $^{94.7}$ S_A $^{143.8}$ I $S_?$ $\swarrow$ 48.8
VII	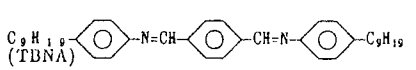	S_G ^{133} S_F $^{154.8}$ S_I $^{156.9}$ S_C $^{192.9}$ S_A $^{198.5}$ I

nesses were not measured, but were estimated to be 0.2 mm thick; they could be visually detected only by reflecting light on the surface of the films.

5. RESULTS AND DISCUSSION

The parameters derived from the X-ray studies of these materials are summarized in Table II.

5.1 Disordered Smectic Phases

The S_A and S_C phases were all confirmed using magnetically aligned samples in Lindemann tubes. The S_C phases were distinguished from the S_A by the tilt of the diffuse area away from the equatorial plane in the diffraction pattern and by lower layer spacings. The tilt angle of the molecules (β_t) was estimated by comparison of the layer spacing (d) and the fully extended molecular length (l) which was obtained from CPK space-filling models.

$$\beta_t = \cos^{-1}(d/l)$$

In the S_A and S_C, this "tilt angle" includes the effects of fluctuations of the long axial direction. The fact that, in the S_A, d is only one or two Angstroms less than "l" suggests that there is no appreciable interdigitation of the molecule in adjacent layers.

5.2 Hexatic Smectic Phases

The hexatic phases in Lindemann tubes showed similar diffraction patterns to the S_A, except that the equatorial reflections were much less diffuse. It was generally not possible to distinguish which phase (S_B, S_F and S_I) was present, because imperfect alignment smeared out the $hk0$ peaks into a continuous area. These samples were used to determine the layer spacing from the $00l$ peaks and the apparent tilt angle β_t. Further information was obtained from diffraction from free-standing films, and the results from all the materials were similar. We will therefore discuss the results only from sample 1 in detail. The diffraction pattern from a free-standing film at 70°C (see Fig. 6*a*) was characteristic of S_I (i.e., tilted towards the apex in real space). On heating the sample gradually (1°C/h) in the absence of the magnetic field, the in-plane scattering profile was observed for the S_C phase (Fig. 6*b*) and the S_A phase (6*c*). The S_C shows an uneven diffuse ring, whereas the S_A gives a uniform ring. The diffuse ring is characteristic of the fluid order within the smectic layer. The unevenness of the diffuse ring occurs as a result of the tilting of the molecular form factor with respect to the plane of the smectic layers which is caused by the tilt of the molecules within the smectic layers. The direction of tilt of the molecules is the same as that observed in the preceding S_I phase. The appearance of the diffuse ring in the S_A phase (Fig. 6*c*) confirms that the smectic layers within the film are oriented parallel to the surface of the brass plate and hence precisely perpendicular to the incident X-ray beam, and so the characteristic pattern in Figure

TABLE II

		S_A		S_C		Hexatic Phase					Crystal Smectic Phases				
	l/Å	*d*/Å	β/degrees	*d*/Å	β_t/degrees	type	*a*/Å	*b*/Å	*c*/Å	β_t/degrees	type	*a*/Å	*b*/Å	*c*/Å	β/degrees
I	38.8	37.6	14	36.0	22	S_I (70°C)	5.4	9.0	38.6	12	—				
II	36.9	36.3	10	35.3	17	S_I (70°C)	5.6	8.9	37.0	16	S_K (55°C)	5.6	8.6	37.3	104 ± 8
III	37.8	36.3	17	35.6	20	S_I (56°C)	5.6	8.9	37.9	20	S_K (51°C)	5.8	8.3	37.9	108
IV	37.8	35.8	19	35.2	21	S_I (87°C)	5.6	8.9	37.9	19	—				
V	36.9	35.4	16	34.6	20	S_I (80°C)	5.5	9.0	36.9	18					
VI	36.7	35.7	14	36.1	10						S_J (82°C)	5.1	8.8	38.1	100
											$S_?$ (35°C)	11.0	17.7	42.0	115 ± 4

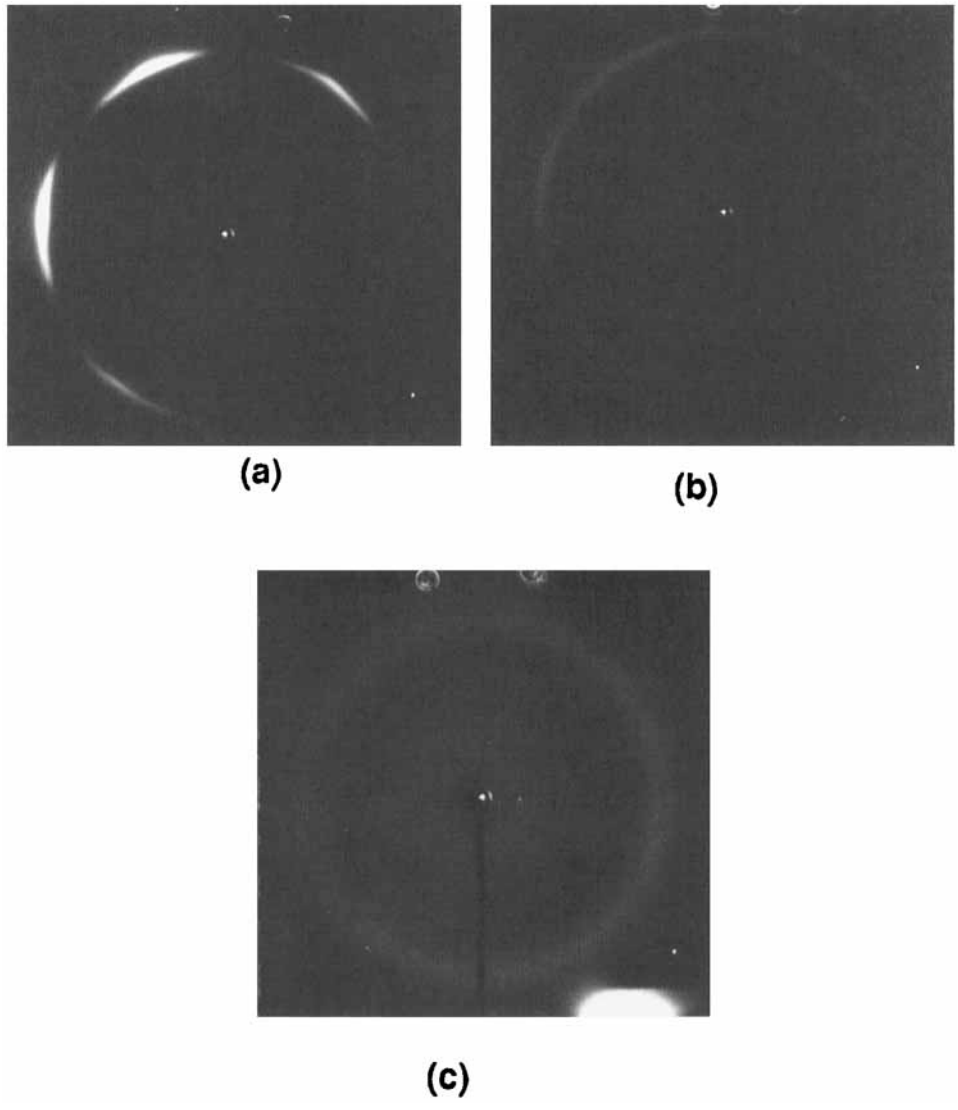

FIGURE 6 X-ray diffraction photographs taken with Cu $K\alpha$ radiation using free-standing films of compound **I**, (*a*) in the S_I phase at 70°C; (*b*) in the S_C phase at 82°C and (*c*) in the S_A phase at 108°C.

6*c* may be taken as proof of the hexatic phase being S_I. The cell parameters in Table II were obtained by assuming the unit cell to be monoclinic with $\beta = 90 + \beta_t$. (The values of β_t were estimated by comparison of d_{001} with the molecular length as for the S_C phases). The *d* spacings for the 001 and 002 peaks from the Lindemann sample were combined with the 110 and 020 from the free standing film.

The other hexatic phases (except for the S_F phase of TBNA) were also identified as S_I. In some cases, the layers in the free-standing film were not parallel to the

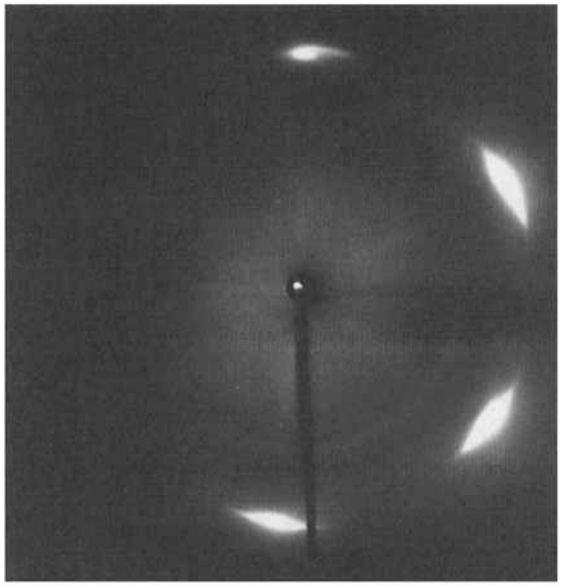

(a)

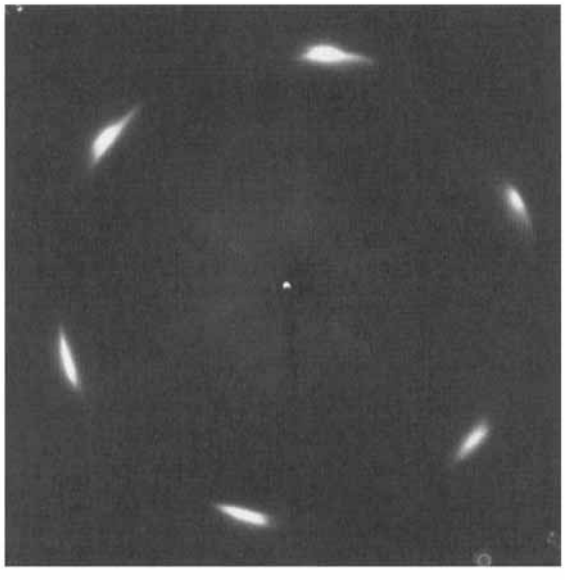

(b)

FIGURE 7 X-ray diffraction photographs of a free-standing film of compound **II** at 70°C in its S_I phase, (*a*) with the beam normal to the layers and (*b*) with the sample rotated by about 15° to show six spots of equal intensity (Cu $K\alpha$ radiation).

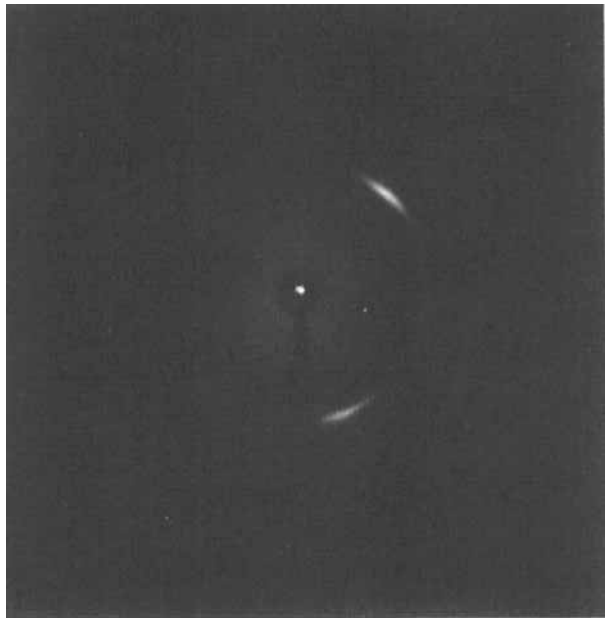

FIGURE 8 X-ray diffraction of a free standing film of TBNA at 137°C in its S_F phase, taken with Mo $K\alpha$ radiation, showing a pattern with a mirror line through the reflection.

supporting plate. When this occurred, the sample was oriented to give six spots of equal intensity and the distortion from the hexagonal symmetry was used to determine which phase was present. For instance, Fig. 7 shows compound **II** in its S_I phase with the film rotated by approximately 15° to be roughly parallel to the molecular axis.

Fig. 8 shows a diffraction pattern from TBNA in the S_F phase. The X-ray beam is normal to the layers and the characteristic pattern (with a mirror plane through a diffraction spot) is observed. In this picture, the mirror plane is nearly horizontal and the value of β_t is such that both diffraction spots on the mirror plane are very weak.

5.3 Crystal Smectic Phases

In these phases, there is long range translational order in all three dimensions, so all the Bragg peaks are sharp.

It was found that in all the samples which exhibited a crystal smectic phase, the unit cell in the smectic phase retained the same tilt direction as the S_I. The S_J and S_K phases were positively identified by indexing the peaks as a monoclinic cell with $b > a$. The peaks were indexed using d spacings from both badly aligned samples in Lindemann tubes and free-standing films. The cell parameters were obtained by least square refinement of a, b, c, and β. The cell parameters were refined to

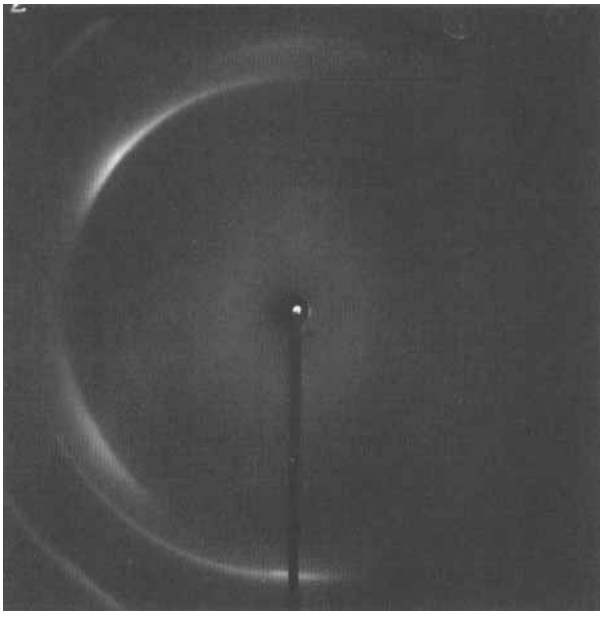

FIGURE 9 X-ray diffraction photograph of compound **III** showing a monodomain S_K phase (Cu $K\alpha$ radiation).

get the best agreement between the observed and calculated d spacings.

$$d_{calc} = \frac{2\pi}{Q_{hkl}}$$

where

$$Q_{hkl} = h^2a^{*2} + k^2b^{*2} + l^2c^{*2} - 2hla^*c^* \cos \beta^*$$

and

$$a^* = \frac{2\pi}{a \sin \beta}; \; b^* = \frac{2\pi}{b}; \; c^* = \frac{2\pi}{c \sin \beta}; \; \beta^* = \pi - \beta.$$

In all cases, it was found possible to get agreement within experimental error for $b > a$ (i.e., a pseudo-hexagonal unit cell tilted towards the apex as in S_J or S_K), but not for $b < a$ (i.e., a unit cell tilted towards an edge as in S_G or S_H). As expected the values of the calculation cell parameter, β, indicate similar tilts to the values of β_t (i.e., $\beta \approx 90 + \beta_t$).

The S_K was distinguished from the S_J phase by the presence of a 120 reflection which indicates that the "c centering" of the unit cell has been lost. In addition the "pseudo-hexagonal" symmetry is lost, so that the relationship:

$$b \approx \sqrt{3}\, a \sin \beta$$

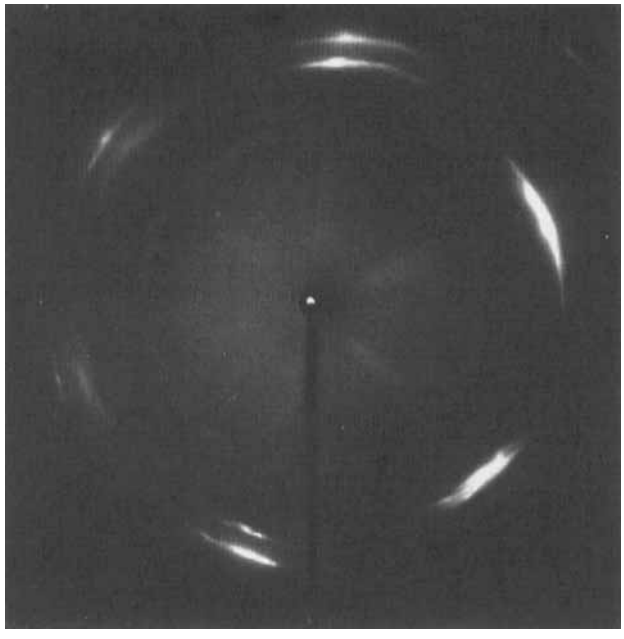

FIGURE 10 X-ray diffraction photograph of compound **II** showing a polydomain S_K phase using Cu $K\alpha$ radiation.

does not hold even approximately, and the 110 and 020 peaks are at well separated Q values.

In compound **III**, the transition from a monodomain S_I to the crystal S_K gave rise to a large in-plane mosaic spread. However, the unit cell retained the same tilt direction as the preceding S_I phase as shown in Fig. 9. The S_K phase in compound **II** appears to have a much narrower mosaic spread, but the sample is no longer a monodomain as shown in Fig. 10. It appears to consist of domains, at three different orientations of the pseudo-hexagonal net in the *ab* plane, where the direction of molecular tilt in the S_I is retained. Fortunately these phases can be identified by indexing the reflections and a monodomain is not essential.

In the S_J phase of compound **VI**, the observed layer spacing was found to be greater than the molecular length l obtained from CPK space-filling models. In our calculation of the unit cell, we have therefore assumed the value from β_t to be the same as that observed in the S_C phase. On cooling the sample to the phase below the smectic J, we observe a doubling of the unit cell along the a and b axes. Unfortunately, only the lower order hkl reflections were observed and this was insufficient to identify the structure of this phase. However, the systematic absence of hkl reflections where $h + k = 2n + 1$, suggest a c-centered monoclinic lattice.

6. CONCLUSIONS

We have successfully identified the smectic phases of a number of liquid crystal materials from monodomain free-standing samples. None of the variations in mo-

lecular structure was able to change the unit cell tilt direction from that of the S_I phase. The method of preparation of the sample is found to be reliable in producing thick, monodomain films. However, success is not guaranteed in every case, as some of the liquid crystals were found to degrade at high temperatures. Furthermore, all the materials studied by us exhibit an $I-S_A$ transition; a different approach may have to be adopted for preparing monodomain free-standing films of other systems. Computer simulations of diffraction patterns of the hexatic phase have shown that it is easy to misinterpret the diffraction pattern if the X-ray beam is not really perpendicular to the smectic layers. Hence, in order to identify a phase, it is required to find a sample orientation which gives six spots of equal intensity and identify the phase by the pattern of the distortion from hexagonal symmetry.

Acknowledgment

We are grateful to Professor G. W. Gray and Dr. D. Lacey for financial support, supply of the samples and for much valuable advice.

REFERENCES

1. D. E. Moncton and R. Pindak, *Phys. Rev. Lett.*, **43**, 701 (1979).
2. R. Pindak, D. E. Moncton, S. C. Davey and J. W. Goodby, *Phys. Rev. Lett.*, **46**, 1135 (1981).
3. R. Pindak, W. O. Sprenger, D. J. Bishop, D. D. Osheroff and J. W. Goodby, *Phys. Rev. Lett.*, **48**, 173 (1982).
4. D. E. Moncton, R. Pindak, S. C. Davey and G. S. Brown, *Phys. Rev. Lett.*, **49**, 1865 (1982).
5. E. B. Sirota, P. S. Pershan, L. B. Sorensen and J. Collet, *Phys. Rev. Lett.*, **53**, 2039 (1985).
6. S. B. Dierker, R. Pindak and R. B. Meyer, *Phys. Rev. Lett.*, **56**, 1819 (1986).
7. J. D. Brock, A. Aharony, R. J. Birgeneau, K. W. Evans-Lutterodt, J. D. Lister, P. M. Horn, G. B. Stephenson and A. R. Tajbaksh, *Phys. Rev. Lett.*, **57**, 98 (1986).
8. S. B. Dierker and R. Pindak, *Phys. Rev. Lett.*, **59**, 1002 (1987).
9. J. Przedmojski and S. Gierlotka, *Liq. Cryst.*, **3**, 409 (1988).
10. S. Gierlotka, J. Przedmojski and B. Pura, *Liq. Cryst.*, **3**, 1535 (1988).
11. P. A. Gane, A. J. Leadbetter, J. J. Bennattar, F. Moussa and A. M. Lambert, *Phys. Rev. A.*, **24**, 2694 (1981).
12. P. A. Gane, A. J. Leadbetter and P. G. Wrighton, *Mol. Cryst. Liq. Cryst.*, **66**, 247 (1981).
13. D. Lacey, private communication.